



Structural Elucidation and Hirshfeld Surface Analysis of A Novel Piperazine Derivative: (4-Benzhydrylpiperazin-1-Yl)(Morpholino)Methanone

**C. S. Ananda Kumar^{1,2}, S. Naveen^{3*}, S. B. Benaka Prasad⁴,
N. S. Linge Gowda⁵ and N. K. Lokanath⁶**

1. Department of Nanotechnology, Visvesvaraya Technological University CPGS, Muddenahalli, Bengaluru region - 562101, **INDIA**
2. Centre for Materials Science, Vijnana Bhavan, University of Mysore, Manasagangotri, Mysuru - 570 006, **INDIA**
3. Institution of Excellence, Vijnana Bhavan Manasagangotri, University of Mysore, Mysuru 570 006, **INDIA**
4. Department of Basic Sciences, School of Engineering and Technology, Jain University, Bengaluru – 562 117, **INDIA**
5. Department of Chemistry, Vidya Vardhaka College of Engineering, Visvesvaraya Technological University, Mysuru 570 002, **INDIA**
6. Department of Studies in Physics, Manasagangotri, University of Mysore, Mysuru - 570 006, **INDIA**

Email: csanandakumar@gmail.com, naveen@ioe.uni-mysore.ac.in

Accepted on 3rd March 2017, Published online on 27th March 2017

ABSTRACT

Title compound was prepared from 1-benzhydryl-piperazine and evaluated for antiproliferative activity and structure was characterized using IR, ¹H-NMR, LC-MS spectra and finally the structure was confirmed by X-ray diffraction studies. The compound crystallizes in the monoclinic crystal system with the space group P2₁/c with both the piperazine and the morpholine rings adopting a chair conformation. The structure exhibits both inter and intramolecular hydrogen bonds of the type C--H...O and contributes to the crystal packing. Further, the Hirshfeld surface analysis reveals the nature of intermolecular contacts; the fingerprint plot provides the information about the percentage contribution from the intermolecular contacts to the surface.

Keywords: 1-Benzhydryl-piperazine, carboxamide, antiproliferative activity, Hirshfeld Surface, C--H...O hydrogen bonds.

INTRODUCTION

The benzhydryl moiety is a fundamental component present in drugs such as antihistamines, antihypertensive, ant Migraine agents and antiallergenic agents [1]. 1-benzhydrylpiperazine bearing dihydronaphthalene derivatives are found to possess excellent pharmacological activities such as vasodilator, hypertensive and cerebral blood flow increasing actions [2]. Diphenyl piperazine derivatives possess broad pharmacological action on central nerves system (CNS), especially on dopaminergic neurotransmission [3]. Piperazine and substituted piperazine are important pharmacophores that can be found in many marked drugs, such as the HIV protease inhibitor Crixivan [4-6] and other drugs namely Cinnarizine, Cetrizine, Cyclizine, Vanoxerine, Elbanizin Flupentixol, Hydroxyzine, and Meclizine. The

synthesis, characterization and antiproliferative activity of the title compound is reported earlier [7]. In view of the above and in continuation of our research on the 1-benzhydryl-piperazine [8-12] derivatives, herein we report the crystal structure studies and Hirshfeld surface analysis of the (4-benzhydrylpiperazin-1-yl)(morpholino)methanone.

MATERIALS AND METHODS

Method of Crystallization: After synthesis and purification [7], the resultant product was allowed to crystallize in ethyl acetate for two days which was left undisturbed. White rectangular crystals grew due to the slow evaporation of ethyl acetate. A schematic diagram of the molecule is shown in figure 1.

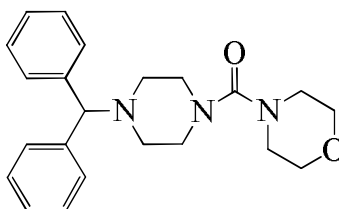


Figure 1: Schematic Diagram of the molecule

Crystal Structure Determination: A single crystal of the title compound with dimensions of 0.25 x 0.2 x 0.15 mm was chosen for X-ray diffraction study. The data were collected on a DIPLabo Image Plate diffractometer equipped with a normal focus, 3 kW sealed X-ray source (graphite-monochromated MoK_α). The crystal to detector distance is fixed at 120 mm with a detector area 441 x 240 mm. Thirty six frames of data were collected at room temperature by the oscillation method. Each exposure of the image plate was set to a period of 400 s. Successive frames were scanned in steps of 5° per min with an oscillation range of 5° . Image processing and data reduction were done using Denzo [13]. The reflections were merged with Scalepack [14]. All of the frames could be indexed using a primitive monoclinic lattice. The structure was solved by direct methods using SHELXS-97 [15]. All of the non-hydrogen atoms were revealed in the first Fourier map itself. The structure was refined by a full-matrix least squares method with anisotropic temperature factors for non-hydrogen atoms using SHELXL-97 [15]. The hydrogen atoms were fixed at chemically acceptable positions and were allowed to ride on their parent atoms. The residuals finally converged to 0.0588. The details of the crystal structure and data refinement are given in table 1. The selected bond lengths and bond angles of the non-hydrogen atoms are given tables 2, 3 respectively. Figure 2 represents the ORTEP of the molecule with thermal ellipsoids drawn at 50% probability.

Table 1: Crystal data and structure refinement details

Parameter	value
CCDC deposit Number	CCDC 1534911
Empirical formula	$\text{C}_{22}\text{H}_{27}\text{N}_3\text{O}_2$
Formula weight	365.47
Temperature	100 (2)K
Wavelength	0.71073 Å
Crystal system, space group	Monoclinic, $P2_1/c$
Unit cell dimensions	$a = 16.9889(16)$ Å $b = 12.1036(9)$ Å $c = 9.3017(8)$ Å $\beta = 93.491(7)^\circ$
Volume	$1909.1(3)$ Å ³
Z	4
Density(calculated)	1.272 Mg m ⁻³
Absorption coefficient	0.082 mm ⁻¹
F_{000}	784
Crystal size	$0.25 \times 0.20 \times 0.15$ mm
θ range for data collection	2.93° to 25.00°

Index ranges	$-19 \leq h \leq 20$ $-14 \leq k \leq 11$ $-10 \leq l \leq 11$
Reflections collected	12469
Independent reflections	3344 [$R_{\text{int}} = 0.0438$]
Refinement method	Full matrix least-squares on F^2
Data / restraints / parameters	3344 / 0 / 245
Goodness-of-fit on F^2	1.022
Final [$I > 2\sigma(I)$]	$R_I = 0.0395$, $wR2 = 0.0877$
R indices (all data)	$R_I = 0.0588$, $wR2 = 0.09861$
Largest diff. peak and hole	0.184 and $-0.205 \text{ e } \text{\AA}^{-3}$

Table 2: Bond Lengths (\AA)

Atoms	Length	Atoms	Length
C1-O1	1.4343(19)	C8-C9	1.515(2)
C1-C2	1.513(2)	C10-C17	1.525(2)
N1-C5	1.3960(19)	C10-C11	1.527(2)
N1-C2	1.4688(19)	C11-C12	1.393(2)
N1-C3	1.4768(19)	C11-C16	1.396(2)
O1-C4	1.4239(18)	C12-C13	1.382(2)
N2-C5	1.369(2)	C13-C14	1.379(2)
N2-C9	1.4611(19)	C14-C15	1.389(3)
N2-C6	1.4665(19)	C15-C16	1.389(2)
O2-C5	1.2332(18)	C17-C18	1.390(2)
C3-C4	1.511(2)	C17-C22	1.398(2)
N3-C7	1.467(2)	C18-C19	1.389(2)
N3-C8	1.4710(19)	C19-C20	1.387(2)
N3-C10	1.480(2)	C20-C21	1.393(2)
C6-C7	1.518(2)	C21-C22	1.387(2)

Table 3: Bond Angles ($^\circ$).

Atoms	Angle	Atoms	Angle
O1-C1-C2	112.08(13)	N2-C9-C8	111.96(14)
C5-N1-C2	115.54(12)	N3-C10-C17	111.01(12)
C5-N1-C3	119.18(12)	N3-C10-C11	109.60(13)
C2-N1-C3	111.31(12)	C17-C10-C11	110.02(12)
C4-O1-C1	109.13(12)	C12-C11-C16	117.98(15)
N1-C2-C1	109.54(13)	C12-C11-C10	121.56(14)
C5-N2-C9	120.17(12)	C16-C11-C10	120.40(15)
C5-N2-C6	124.42(13)	C13-C12-C11	121.59(15)
C9-N2-C6	114.40(12)	C14-C13-C12	119.83(16)
N1-C3-C4	109.03(13)	C13-C14-C15	119.82(16)
C7-N3-C8	107.90(12)	C16-C15-C14	120.14(17)
C7-N3-C10	114.49(13)	C15-C16-C11	120.63(16)
C8-N3-C10	110.85(12)	C18-C17-C22	118.32(15)
O1-C4-C3	111.07(12)	C18-C17-C10	120.97(14)
O2-C5-N2	122.59(14)	C22-C17-C10	120.71(14)
O2-C5-N1	121.61(14)	C19-C18-C17	120.99(16)
N2-C5-N1	115.79(13)	C20-C19-C18	120.20(16)
N2-C6-C7	110.60(13)	C19-C20-C21	119.50(16)
N3-C7-C6	109.58(13)	C22-C21-C20	120.00(16)
N3-C8-C9	110.26(13)	C21-C22-C17	120.98(16)

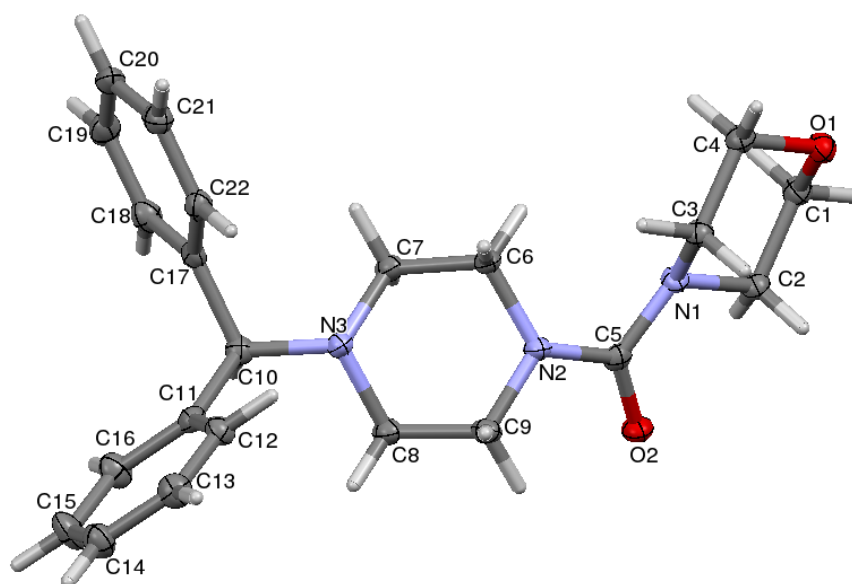


Figure 2: ORTEP of the molecule with thermal ellipsoids drawn at 50% probability.

RESULTS AND DISCUSSION

A study of the torsion angles, asymmetric parameters and least-squares plane calculations reveals that the piperazine ring in the structure adopts a chair conformation with the atoms N2 and N3 lying 0.1633(14) Å and 62.37(16) Å respectively from the Cremer and Pople plane [16] defined by the atoms N2/N3/C6/C7/C8/C9. This is confirmed by the puckering parameters $Q = 0.5700(16)$ Å, $\theta = 11.61(15)^\circ$ and $\varphi = 167.1(8)^\circ$. The ring puckering analysis revealed that the piperazine ring has a weighted average ring bond distance of 1.4826(8,105) Å and a weighted average torsion angle of 56.48(7, 279)°. The sum of the bond angles around the piperazine N atoms N2 and N3 are 336.96° and 311.52° indicating that they are SP^3 hybridized and thus adopt a pyramidal geometry [17]. The bond N2-C5 connecting the morpholine ring and the piperazine ring makes an angle of 53.57(10)° with the Cremer and Pople plane of the piperazine ring and thus bisects the plane of the piperazine ring whereas the bond N3-C10 connecting both the phenyl rings makes an angle of 80.71(9)° with the Cremer and Pople plane of the piperazine ring and thus lies in the equatorial plane of the piperazine ring. Also, a study of the torsion angles, asymmetric parameters and least-squares plane calculations reveals that the morpholine ring in the structure adopts a chair conformation with the atoms O1 and N1 lying 0.2473(12) Å and -0.2198(14) Å respectively from the Cremer and Pople plane defined by the atoms O1/N1/C1/C2/C3/C4. This is confirmed by the puckering parameters $Q = 0.5729(16)$ Å, $\theta = 3.19(16)^\circ$ and $\varphi = 319(3)^\circ$. The ring puckering analysis revealed that the morpholine ring has a weighted average ring bond distance of 1.4713(8,153) Å and a weighted average torsion angle of 57.68(7, 118)°. The sum of the bond angles around the morpholine O and N atoms O2 and N1 are 332.27° and 329.88° indicating that they are SP^3 hybridized and thus adopt a pyramidal geometry. The bond N1-C5 connecting the morpholine ring and the piperazine ring makes an angle of 87.06(10)° with the Cremer and Pople plane of the piperazine ring and thus lies in the equatorial plane of the morpholine ring. The steric hindrance caused by the morpholine ring is more than the steric effects caused by the diphenyl rings which is evident from the bond angle values of 114.40(12)° and 107.90(12)° for C6-N2-C9 and C7-N3-C8 respectively. The dihedral angle between the piperazine ring and the morpholine ring is 68.91° whereas the dihedral angle between the piperazine ring and the two phenyl rings C11-C5 and C17-C22 are 66.61(8)° and 71.29(8)° respectively. The dihedral angle between the morpholine ring and the two phenyl rings C11-C5 and C17-C22 are 45.63(8)° and 78.51(8)° respectively whereas the two phenyl rings make a dihedral angle of 73.38(8)° with each other. The structure exhibits both inter and

intramolecular hydrogen bonds of the type C—H...O and C—H...N. The intermolecular hydrogen bond between the carbonyl group and the carbon atom of the morpholine ring has a length of 3.364(2) Å and makes an angle of 149° with a symmetry code $x, 3/2-y, 1/2+z$. This hydrogen bond links the molecule to form a one-dimensional chain when viewed along the b axis (**Figure 3**). The packing of the molecules when viewed along the c axis indicate that the molecules exhibit layered stacking and are connected by the hydrogen bonds to form a three dimensional structure (**Figure 4**).

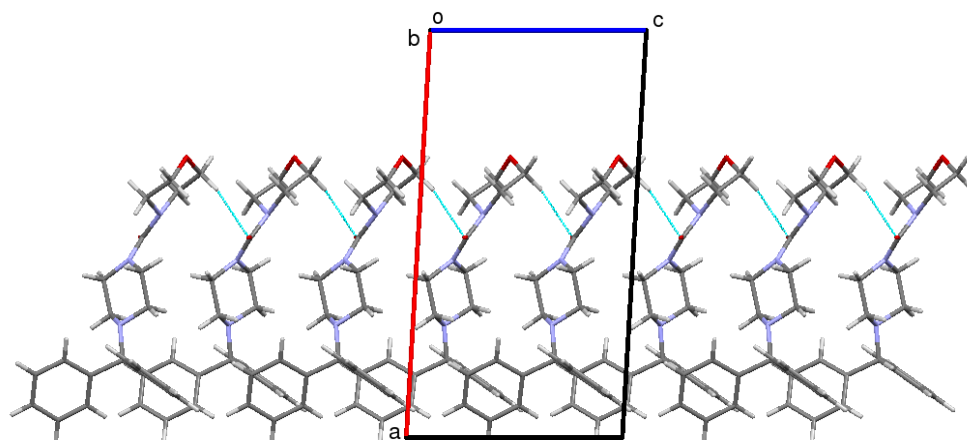


Figure 3: Packing of the molecules when viewed down along the b axis. The blue dotted lines represent intermolecular hydrogen bonds

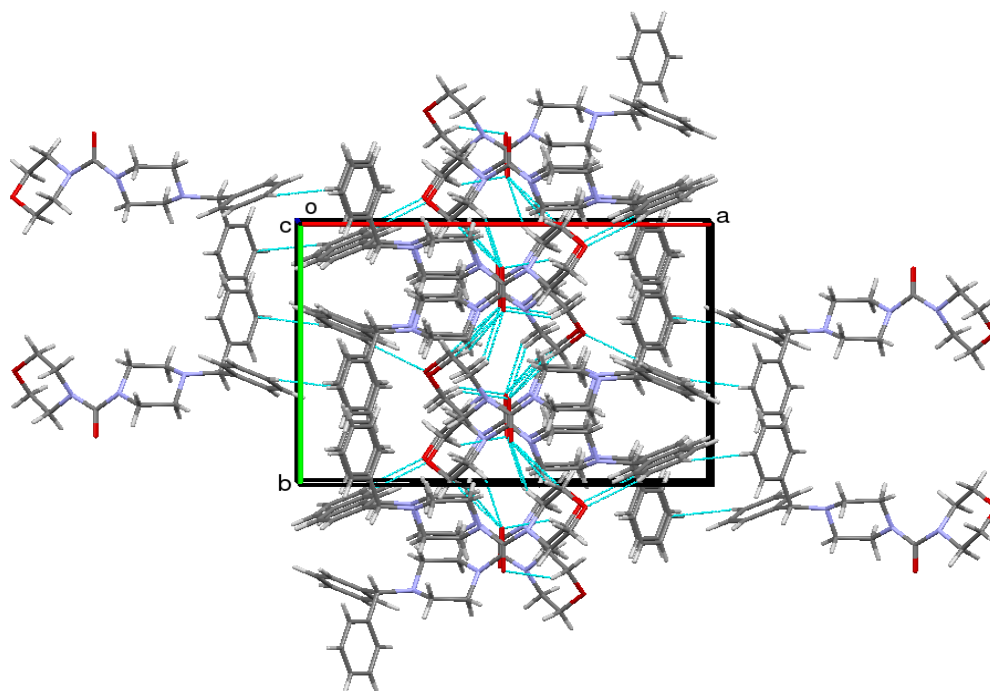


Figure 4: Packing of the molecules when viewed down along the c axis exhibiting layered stacking. The blue dotted lines represent intermolecular hydrogen bonds.

Hirshfeld surface analysis: The program Crystal Explorer 3.0 [18] was used to perform Hirshfeld surfaces computational analysis and to quantify the intermolecular interactions in terms of surface

contribution and generating graphical representations, plotting 2D fingerprint plots [19-20], and generating electrostatic potential [21] with TONTO [22]. The electrostatic potential was mapped on Hirshfeld surfaces using Hartree-Fock (STO-3G basis set) theory over the range of -0.020 a.u. to $+0.020$ a.u. The electrostatic potential surfaces are plotted with red region which is a negative electrostatic potential (hydrogen acceptors) and blue region which is a positive electrostatic potential (hydrogen donor).

Hirshfeld surface analysis is an effective tool for exploring packing modes and intermolecular interactions in molecular crystals, as they provide a visual picture of intermolecular interactions and of molecular shapes in a crystalline environment. Surface features characteristic of different types of intermolecular interactions can be identified, and these features can be revealed by color coding distances from the surface to the nearest atom exterior (d_e plots) or interior (d_i plots) to the surface. This gives a visual picture of different types of interactions present and also reflects their relative contributions from molecule to molecule. Further, 2D fingerprint plots (FP), in particular the breakdown of FP into specific atom...atom contacts in a crystal, provide a quantitative idea of the types of intermolecular contacts experienced by molecules in the bulk and presents this information in a convenient color plot. Hirshfeld surfaces comprising d_{norm} surface and Finger Print plots were generated and analyzed for the title compound in order to explore the packing modes and intermolecular interactions. The two dimensional fingerprint plots from Hirshfeld surface analyses **figure 5**, illustrates the difference between the intermolecular interaction patterns and the relative contributions to the Hirshfeld surface (in percentage) for the major intermolecular contacts associated with the title compound. The fingerprint plots can be decomposed to highlight particular atoms pair close contacts. There are two sharp spikes pointing toward the lower left of the plots and are typical C--H...O hydrogen bonds. Importantly, H...H (70.4%) bonding appears to be a major contributor in the crystal packing, whereas the C...H/H...C (16.4%), and O...H/H...O (11.9%) plots also reveal the information regarding the intermolecular hydrogen bonds thus supporting for the intermolecular interactions. This intermolecular contact is highlighted by conventional mapping of d_{norm} on molecular Hirshfeld surfaces and is shown in **figure 6**. The red spots over the surface indicate the intercontacts involved in hydrogen bond. The dark-red spots on the d_{norm} surface arise as a result of the short interatomic contacts, i.e., strong hydrogen bonds, while the other intermolecular interactions appear as light-red spots.

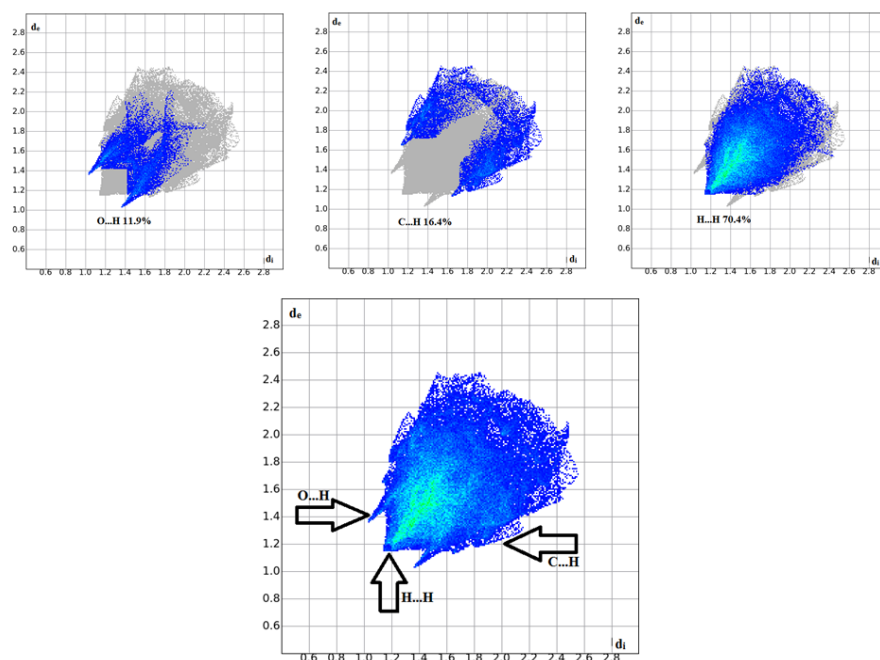


Figure 5: Fingerprint plots of the title compound showing H...H, C...H & O...H interactions. d_i is the closest internal distance from a given point on the Hirshfeld surface and d_e is the closest external contacts

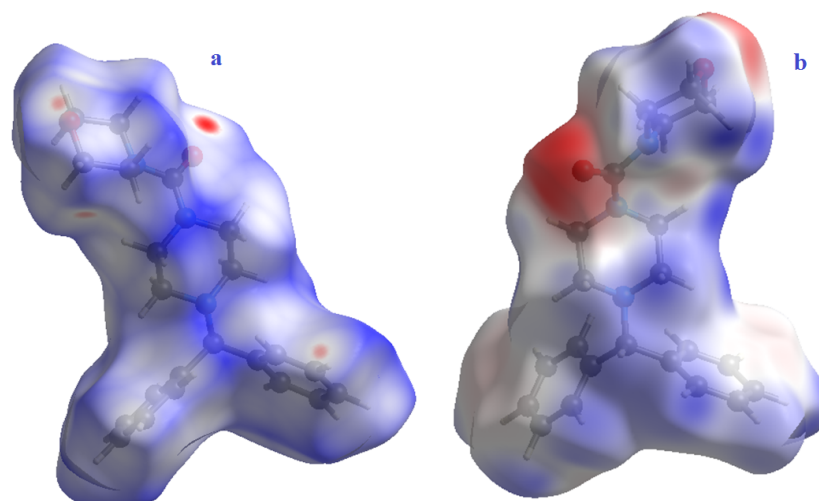


Figure 6: (a) d_{norm} and (b) electrostatic potential mapped on Hirshfeld surface for visualizing the intermolecular contacts.

REFERENCES

- [1] Ferrer International. S.A., *US-4883797.*, **1989**.
- [2] O. Yoshikazu, I. Katsumi, H. Minoru, *US patent*, **1980**, 4, 582.
- [3] M. Kimura, T. Masuda, K. Yamada, M. Mitani, N. Kubota, N. Kawakatsu, K. Kishii, M. Inazu, Y. Kiuchi, K. Oguchi, T. Namiki, *Bioorg. Med. Chem.*, **2003**, 11, 3953.
- [4] J. P. Vacca, B. D. Dorsey, W. A. Schleif, R. B. Levine, S. L. McDaniel, P. L. Darke, J. Zugay, J. C. Quintero, O. M. Blahy, B. B. Sardana, A. J. Schlabach, P. I. Graham, J. H. Condra, L. Gotalib, M. K. Holloway, J. Lin, L. W. Chen, K. Vastag, D. Ostovic, P. S. Anderson, E. A. Emini, J. R. Hu, *J. Med. Chem.*, **1994**, 37, 3443.
- [5] D. Askin, K. K. Eng, K. Rossen, R. M. Purick, K. M. Wells, R. P. Volante, P. J. Reider, *Tetrahedron Lett.*, **1994**, 35, 673.
- [6] K. Rossen, S. A. Weissman, J. Sagar, A. Reamer, D. A. Askin, R. P. Volante, P. J. Reider, *Tetrahedron Lett.*, **1995**, 36, 6419.
- [7] C. S. Ananda Kumar, S.B. Benaka Prasad, K. Vinaya, S. Chandrappa, N.R. Thimmegowda, Y.C. Sunil Kumar, Sanjay Swarup, K.S. Rangappa, *Eur. J. Med. chem.*, **2009**, 44, 1223-1229.
- [8] C. S. Ananda Kumar, S. Nanjunda Swamy, N. R. Thimmegowda, S. B. Benaka Prasad, George W. Yip, K. S. Rangappa, *Med. Chem. Res*, **2007**, 16, 179–187.
- [9] C.S. Ananda Kumar, K. Vinaya, J. Narendra Sharath Chandra, N.R. Thimmegowda, S.B. Benaka Prasad, C.T. Sadashiva, K.S. Rangappa, *J. Enzy. Inhi. Med. Chem*, **2008**, 23, 462-469.
- [10] C.S. Ananda Kumar, H. Chandru, A.C. Sharada, N.R. Thimmegowda, S.B. Benaka Prasad, M. Karuna Kumar, K.S. Rangappa, *Med. Chem*, **2008**, 4, 466.
- [11] S. Naveen, C. S. Ananda Kumar, H. R. Manjunath, K. Vinaya, S. B. Benaka Prasad, M. A. Sridhar, K. S. Rangappa J. Shashidhara Prasad, *Mol. Cry. Liq. Cryst*, **2009**, 503, 151.
- [12] C. S. Ananda Kumar, S. Naveen, S. B. Benaka Prasad, N. R. Thimmegowda, N. S. Lingegowda, M. A. Sridhar, J. Shashidhara Prasad, K. S. Rangappa, *J. Chem. Cryst.*, **2007**, 37, 727.
- [13] Z. Otwinowski, W. Minor, *Macromolecular Crystallography 276 part A*, 307; ed. Carter Jr, C.M., Sweet, R.M. Academic Press, New York.

- [14] S. Mackay, C. J. Gillmore, C. Edwards, K. Shankland, **1999**, maXus, Computer program for the solution and refinement of crystal structures; Bruker Nonius, MacScience, Japan and the University of Glasgow, Netherlands.
- [15] G. M. Sheldrick, SHELXS-97 & SHELXL-97, **1997**.
- [16] D. Cremer, J. A. Pople, *J. Amer. Chem. Soc.*, **1975**, 97, 1354.
- [17] A. Perales, F. H. Cano, S. Garcia-Blanco, *Acta Cryst.*, B33, 1977, 3172.
- [18] S. K. Wolff, D. J. Grimwood, J. J. McKinnon, M. J. Turner, D. Jayatilaka, M. A. Spackman, *CrystalExplorer* (Version 3.0), *University of Western Australia*, **2012**.
- [19] Saikat Kumar Seth, *Cryst. Engg. Comm.*, **2013**, 15, 1772.
- [20] Saikat Kumar Seth, *J. Mol. Struct.*, **2014**, 1064, 70.
- [21] M. A. Spackman, J. J. McKinnon, D. Jayatilaka, *Cryst. Engg. Comm.*, **2008**, 10(4), 377.
- [22] D. Jayatilaka, D. J. Grimwood, A. Lee, A. Lemay, A. J. Russel, C. Taylor, S. K. Wolff, TONTO—A System for Computational Chemistry, The University of Western Australia, Nedlands, Australia, **2005**.

AUTHORS' ADDRESSES

1. **Prof. N. K. Lokanath**

Department of Studies in Physics
University of Mysore, Mysore, India-570006
Email: lokanath@physics.uni-mysore.ac.in, Mobile: +91-9449806412

2. **Dr. C. S. Ananda Kumar**

Department of Nanotechnology, Visvesvaraya Technological University, CPGS,
Muddenahalli, Bengaluru region - 562101, India
Centre for Materials Science, Vijnana Bhavan, University of Mysore,
Manasagangotri, Mysore - 570 006, India
Email: csanandakumar@gmail.com, Mobile: +91-9741264513

3. **Dr. S. Naveen**

Scientist, Institution of Excellence, University of Mysore, Mysore, India-570006
Email: naveenxrd@gmail.com, Mobile: +91-9845873377

4. **Dr. S. B. Benaka Prasad**

Associate Professor in Chemistry and HOD, Department of Basic Science, School of Engineering and
Technology, Jain University Bangalore, India
Email: benakaprasad@gmail.com, Mobile: +91-9986982138

5. **Dr. N. S. Lingegowda**

Department of Chemistry, Vidyavardhaka College of Engineering,
Visvesvaraya Technological University, Mysore 570 002
Email: nslgowda@vvce.ac.in, Mobile: +91-9845790255